#341

# Tropical Agricultural Hydrology

## WATERSHED MANAGEMENT AND LAND USE

Edited by
R. Lal
and
E. W. Russell

# *Tropical Agricultural Hydrology*

## Watershed Management and Land use

*Edited by*

**R. Lal**
*International Institute of Tropical Agriculture,*
*Ibadan, Nigeria*

and

**E. W. Russell**
*Professor Emeritus of the Department of Soil Science,*
*University of Reading*

*A Wiley-Interscience Publication*

JOHN WILEY & SONS
Chichester · New York · Brisbane · Toronto

The papers in this volume were initially presented at a Conference organized by the International Institute of Tropical Agriculture, Ibadan, Nigeria, in November 1979

Tropical Agricultural Hydrology
Edited by R. Lal and E. W. Russell


# 6.1

# Simulation of Erosion and Sediment Yield from Field-sized Areas

G. R. FOSTER AND L. J. LANE

## 6.1.1. INTRODUCTION

A method is needed to evaluate sediment yield from field-sized areas under various management practices to control non-point-source pollution. In response to this need, we developed a reasonably simple simulation model that incorporates fundamental principles of erosion, deposition, and sediment transport mechanics.

Sediment load in overload flow and open channel flow is controlled by either transport capacity or sediment available for transport. If sediment load is less than transport capacity, detachment can occur, and deposition occurs when sediment load exceeds the transport capacity. The model provides comprehensive representation of a field by considering complex overland flow slopes, concentrated channel flow, and impoundments or ponds. The model estimates transport of sediment composed of primary particles (sand, silt, and clay) and large and small aggregates. In deposition, sediment sorting is calculated which can result in enrichment of the finer particles.

Sediment yield is a function of sediment production by erosion and the subsequent transport of the sediment. On a given field, either erosion or sediment transport capacity may limit sediment yield, depending on topography, soil characteristics, cover, and rainfall–runoff rates and amounts. The controlling mechanism can change from season to season, from storm to storm, and even within a storm. The relationships for erosion and transport are different, which prevents lumping them into a single equation. Since erosion and transport for each storm are best considered separately, lumped equations such as the Universal Soil Loss Equation, USLE, (Wischmeier and Smith, 1978), or Williams' (1975) modified USLE (a flow transport–sediment yield equation) cannot give the best results over a broad range of conditions on field-sized areas. Furthermore, the interrelation between erosion and transport is non-linear and interactive for each storm, which prevents using separate equations to linearly accumulate erosion or sediment transport capacity over several storms. Therefore, to simulate erosion and sediment yield on an individual storm basis and to satisfy the need for a continuous simulation model, we selected a more fundamental approach with separate equations used for erosion and sediment transport.

Several fundamentally based models (e.g. Beasley *et al.*, 1977; Li, 1977) compute erosion and transport at various times during the runoff event. Although these models are powerful, they require excessive use of computer time which practically prohibits simulating 20 to 30 years of record. The model described herein uses characteristic rainfall and runoff factors for a storm to compute erosion and sediment transport for that storm. In terms of computational time, this corresponds to a single time step for models which simulate over the entire runoff event.

The model is intended to be useful without calibration or collection of research data to determine parameter values. Therefore, established relationships, such as the USLE, were modified and used in the model.

## 6.1.2. BASIC STRUCTURE OF MODEL

The erosion–sediment yield model is a component of a more comprehensive model consisting of hydrologic, erosion, nutrient, and pesticide components (Knisel, 1978). Briefly, the erosion component receives as input from the hydrologic model rainfall and runoff data and provides input to the chemical transport components. This paper describes the erosion–sediment yield component of the more comprehensive model.

### 6.1.2.1. Basic Processes

The model was developed for quasi-steady state conditions by using characteristic measures for hydrologic inputs. Rainfall is described by volume and the product of storm energy and maximum 30-minute intensity. Volume and peak rate attenuated for travel time are used to describe runoff. These terms drive soil detachment and subsequent transport in overland and open channel flow.

The principal governing equation is the continuity equation expressed as:

$$\frac{dG}{dx} = D_L + D_F \tag{6.1}$$

where $G$ is sediment load, $x$ is distance, $D_L$ is the rate of lateral inflow of sediment, and $D_F$ is the rate of sediment removal (deposition) or addition (detachment). Equation (6.1) applies to overland flow and flow in channels. The flow path is divided into segments and equation (6.1) is applied sequentially to each segment.

The minimum potential sediment load at the lower end of a segment is the sum of incoming sediment at the upper end of the segment and that added by lateral inflow within the segment. This potential load is compared with sediment transport capacity. If sediment transport capacity exceeds the potential load, the potential exists for detachment by flow. The detachment rate will be the lesser of the detachment rate to satisfy transport capacity or the detachment capacity of the flow. When soil is detached by flow, it adds particles whose distribution is specified in the input data. On overland flow areas, lateral inflow of sediment is from inter-rill erosion and has the input distribution. Lateral inflow of sediment into the channels is from overland flow or other channels. This sediment has the distribution from the sediment yield calculations.

If the potential sediment load exceeds transport capacity, deposition occurs at the rate of:

$$D = \alpha(T_c - G) \tag{6.2}$$

where $D$ is deposition rate (mass area$^{-1}$ time$^{-1}$), $\alpha$ is a first order reaction coefficient (length$^{-1}$), and $T_c$ is transport capacity (mass width$^{-1}$ time$^{-1}$). The coefficient $\alpha$ is estimated from:

$$\alpha = E\, V_s / q \tag{6.3}$$

where $E$ is 0.5 for overland flow (Davis, 1978), and 1.0 for channel flow (Einstein, 1968), $V_s$ is particle fall velocity, and $q$ is water discharge per unit width, Since $\alpha$ is large for coarse and heavy particles, they deposit rapidly, leaving the sediment relatively enriched in smaller and lighter particles. Also, the transport capacity equation considers the transportability of particles with various sizes and densities.

These equations are solved in the same way for both overland and channel flow. However, detachment by flow is computed differently for overland and channel flow.

#### 6.1.2.2. Overland Flow

To describe sediment detachment by raindrop impact and inter-rill and rill flow, a modification of the Universal Soil Loss Equation is used for individual storm events. Inter-rill detachment ($D_{IR}$) in the overland flow element is expressed as

$$D_{IR} = 4.57\, EI(S + 0.014)KCP(q_p/Q) \tag{6.4}$$

where $EI$ is storm rainfall energy times maximum 30 minute intensity, $S$ is overland flow slope, $q_p$ is peak rate of runoff, $Q$ is runoff volume, $K$ is the soil erodibility factor, $C$ is the cover-management factor, and $P$ is the supporting practice factor. Notice that $D_{IR}$ is equivalent to $D_L$ in equation (6.1). The rill detachment process is described by

$$D_R = (6.86 \times 10^6) n_x Q q_p^{1/3} (x/22.1)^n x^{-1} S^2 KCP(q_p/Q) \tag{6.5}$$

where $D_R$ is the rill detachment rate, $n_x$ is the slope length exponent, $x$ is the distance downslope, and the other variables are as described above. Only the USLE contouring part of the $P$ factor is used. The model is structured to directly account for other highly variable USLE $P$-factors such as strip cropping and deposition in terrace channels.

Sediment transport capacity is calculated using the Yalin sediment transport equation (Yalin, 1963). Sediment transport capacity, $W_s$, in units of mass time$^{-1}$ flow-width$^{-1}$ is calculated using

$$W_s = 0.635\, \delta\, V_* s \rho_w d\left[1 - \frac{1}{\sigma}\log(1+\sigma)\right] \tag{6.6}$$

where:

$$\sigma = A\delta \tag{6.7}$$

$$A = 2.45 s^{-0.4}(Y_{cr})^{0.5} \tag{6.8}$$

$$\delta = \begin{cases} 0 & Y < Y_{cr} \\ \dfrac{Y}{Y_{cr}} - 1 & Y > Y_{cr} \end{cases} \tag{6.9}$$

$$Y = \frac{V_*^2}{(s-1.0)gd}, \text{ and} \tag{6.10}$$

$$V_* = (gRS_f)^{1/2} = (\tau/\rho_w)^{1/2} \tag{6.11}$$

With this notation, $V_*$ is the shear velocity, $\tau$ is the shear stress, $g$ is acceleration of gravity, $R$ is hydraulic radius defined as the cross-sectional area divided by the wetted perimeter, $S_f$ is the friction slope, $s$ is particle specific gravity, $d$, is particle diameter, $Y_{cr}$ is the critical lift force from the Shields' diagram extended to low particle Reynolds numbers, and $\rho_w$ is the mass density of the fluid. The constant 0.635 and the Shields' diagram were empirically derived. Shear stress required for the Yalin equation is computed using the Manning equation.

The sediment load may have fewer particles of a given type than the flow's transport capacity for that type. At the same time, the sediment load of other particle types may exceed the flow's transport capacity for those types. The excess transport capacity for the deficit types is assumed to be available to increase the transport capacity for the types where available sediment exceeds transport capacity.

The Yalin equation was modified to shift excess transport capacity. For large sediment loads (sediment loads for each particle type clearly in excess of the respective transport capacity for each particle type), or for small loads (sediment loads for each particle type clearly less than the respective transport capacity for each particle type), the flow's transport capacity is distributed among the available particle types based on particle size and density and flow characteristics.

### 6.1.2.3. Concentrated Flow

The concentrated flow or channel element of the erosion model assumes that peak rate of runoff is the characteristic discharge for the channel, and detachment-deposition is based on that discharge. Detachment can occur when the shear stress developed by the characteristic discharge is greater than the critical shear stress for the channel. Bare channels, grassed waterways, and combinations of bare and grass channels can be considered by the model with as many as 10 channel segments. Discharge is assumed to be steady state, but spatially varied, increasing downstream with lateral inflow. Friction slope and shear stress are estimated from solution of the spatially varied flow equations. The solutions consider draw-down or backwater effects in the channel as a result of channel outlet control.

The concentrated flow relationships discussed here are limited to upland areas typical of farm-field situations and include: (1) erosional channel development in areas of fields where flow is concentrated such as stream headwaters, terrace channels, etc., (2) small channels as permanent features of the landscape which are normally 'tilled over' during cultivation, and (3) temporary channels developing when rows or terraces overtop and flow proceeds cross-contour to the field edge. Specifically excluded are permanent stream channels and active gully systems of a scale larger than described above. Such large-scale features are more in the range of a basin-scale model than the field-scale model. Finally, gully systems are beyond the scope of the current field-scale modelling effort due to our lack of understanding of gully dynamics. An exception to the channel size limitations is in development of a final or equilibrium channel width. As discussed below, relationships developed for field-sized channels also apply to larger channels.

Hydrologic inputs to the channel system consist of overland flow hydrographs or volume and peak rate of runoff and a duration of runoff. In the latter case, it is necessary to choose a characteristic discharge and a time distribution with the specified peak, volume, and duration. In this analysis, we assumed that the peak rate is the characteristic discharge, and that the temporal distribution of shear stress in the channel is triangular.

Given the hydrologic input to the channel system, the next step was to apply equations (6.1)–(6.2) with the same logic as used for the overland flow areas. Lateral inflow of sediment is from overland flow or contributing channels and $D_f$ is erosion or deposition in the channel.

An estimate of shear stress along the channel was required. The routing equations were simplified by using the peak or characteristic discharge with the assumption of steady flow. This eliminated the unsteady flow equations, leaving steady but spatially varied flow.

As described by Chow (1959), the dynamic equation for spatially varied flow with increasing discharge is

$$\frac{dy}{dx} = \frac{S_0 - S_f - 2\alpha Q q_* / gA^2}{1 - \alpha Q^2 / gA^2 D} \qquad (6.12)$$

where

$\frac{dy}{dx}$ = slope of water surface,

$S_0$ = bed slope,

$S_f$ = friction slope,
$\alpha$ = energy coefficient,
$Q$ = discharge at point of interest,
$q_*$ = lateral inflow per unit length of channel,
$A$ = cross-sectional area,
$D$ = hydraulic depth, and
$g$ = acceleration due to gravity.

To avoid solving equation (6.12) for each runoff event, it was solved under a variety of conditions, and regression equations were used to approximate the solutions (Foster *et al.*, 1980). Given a representative channel and flow conditions, we derived regression equations for the friction slope as a function of position along the channel. Given the friction slope $S_f(x)$, the average shear stress at distance $x$ downstream is then

$$\tau(x) = \gamma R(x) S_f(x) \tag{6.13}$$

where:

$\tau(x)$ = shear stress, force per unit area,
$\gamma$ = specific gravity of water, and
$R(x)$ = hydraulic radius, length.

In many field situations, outlet control for a channel has a significant influence on sediment detachment and transport capacity. Consequently, back-water or drawdown at the outlet can significantly affect sediment yield. If the outlet rating is known (critical depth or a rating table), then the friction slope at the outlet is

$$S_f = \frac{n^2 Q^2}{A^2 R^{4/3}} \tag{6.14}$$

where $n$ is Manning's resistance coefficient. Subsequent values of friction slope at positions above the outlet are obtained from the spatially varied flow equation (equation (6.14)) or the approximating regression equations. The procedure is similar to computation of backwater profiles except that spatially varied flow is considered.

Solutions for equations (6.12)–(6.14) are used to derive $S_f$ and which are required to solve the detachment capacity equation, the Yalin equation, and equations (6.1)–(6.3). The following discussion emphasizes the detachment capacity equations developed for and used in the model.

The detachment equations are based on a simplified channel morphology–erosion–sediment yield model. Objectives of this simplified model included developing equations which would: (1) be relatively simple with a minimum number of parameters, (2) incorporate what is known of channel hydraulics, (3) reproduce observed relationships between sediment yield and time for developing channel systems. Limiting assumptions were: (1) steady-state discharge, (2) erosion occurs at potential rate (no depositional-erosional cycles), and (3) the shear stress distribution around the wetted perimeter can be approximated using data from rectangular channels. Moreover, the quasi-steady state morphological relationships could be tested using existing channels, but the dynamic relationships require data from developing, dynamic channel systems.

The model simulates channel development in homogeneous-erodible material and in material with an erosion-resistant or 'non-erodible' boundary. Input to the model consists of a flow rate $Q$, a channel slope $S$, hydraulic resistance parameter $n$, soil erodibility factor $K_{ch}$, a critical shear stress $\tau_{cr}$, and parameters for the shear stress distribution around the channel cross-section. If a non-erodible boundary is present, then the depth to this boundary, $d_{side}$, is also required.

Detachment rate was assumed to be given by:

$$D_p = K_{ch}(\tau - \tau_{cr})^c \tag{6.15}$$

where $D_p$ is detachment rate at a point along the wetted perimeter, $K_{ch}$ is a soil erodibility factor for channel erosion, $\tau$ is shear stress at a point along the wetted perimeter, $\tau_{cr}$ is a critical shear stress, and $c$ is an exponent. Under a continuous steady discharge, the channel reaches an equilibrium width, $W_{ac}$, that moves downward at the rate that the middle of the channel erodes. Although the actual cross-sections are irregular and dynamic in an eroding channel, as a first approximation we assume a rectangular cross-section with specified width. This width is given by:

$$W_{ac} = \left[\frac{nQ}{S^{1/2}}\right]^{3/8} \frac{W_*}{R_*^{\ 5/8}} \tag{6.16}$$

where $W_*$ and $R_*$ are geometric properties that depend on the shear stress distribution $\tau_{cr}$, $Q$, $n$, and $S$. The functions for $W_*$ and $R_*$ were numerically derived. The corresponding erosion rate $E_0$ is

$$E_0 = W_{ac}K_{ch}(1.35\bar{\tau} - \tau_{cr})^c \tag{6.17}$$

where $\bar{\tau}$ is the average shear stress in the cross section, 1.35 is the ratio of the maximum to the average shear stress in small rectangular channels, and $c$ is an exponent with a value of 1.05 to 1.10.

When the channel reaches the non-erodible layer, downward movement of the channel ceases and the channel widens. As it widens, erosion rate decreases. The channel continues to widen until the shear stress at the non-erodible layer equals the critical shear stress. The final width at which erosion ceases is:

$$W_f = \left[\frac{nQ}{S^{1/2}}\right]^{3/8} \left[\frac{1 - 2x_*}{x_*^{\ 5/8}}\right]^{3/8} \tag{6.18}$$

where $x_*$ is the normalized distance from the water surface to where $\tau$ equals $\tau_{cr}$ divided by the wetted perimeter. The final width $W_f$ is a function of the distribution of $\tau$, $\tau_{cr}$, $Q$, $n$, and $S$.

The erosion rate immediately after the channel reaches the non-erodible boundary is:

$$E_1 = 2K_{ch}(\tau_b - \tau_{cr})^c d_{soil} \tag{6.19}$$

where $\tau_b$ is the shear stress at the non-erodible boundary and $d_{soil}$ is the depth of the soil above the non-erodible layer.

Once the non-erodible boundary is reached but before the final eroded width is reached, erosion rates decrease exponentially with time as

$$E(t) = E_i \exp(-\alpha t_*) \tag{6.20}$$

where $E(t)$ is erosion rate with time, $\alpha$ is a decay constant, and $t_*$ is the normalized time. This normalized time $t_*$ is computed from

$$t_* = tE_i/[(W_f - W_{ac})d_{soil}\rho_{soil}] \tag{6.21}$$

where $t$ is time since the non-erodible boundary is reached, $E_i$ is the initial erosion rate from equation (6.20), $W_f$ is the final eroded width from equation (6.18), $W_{ac}$ is the equilibrium width from equation (6.16), and $\rho_{soil}$ is the apparent mass density of the soil.

Equations (6.16)–(6.21) provide a means of computing widths and associated erosion rates for eroding channels in homogeneous soil and under circumstances where a non-erodible boundary is present.

### 6.1.2.4. Impoundment Component

Impoundments often occur in field situations, either where a channel flows through a restriction (for instance a fence line or a road culvert) or in an impoundment-type terrace. Any such restriction reduces the flow velocity giving coarse-grain sediments and aggregates an opportunity to settle out of the flow. Deposition in impoundments is a function of the fall velocity of the particles and travel time through the impoundment. The fraction of particles, $FP$ of a given size, $i$, is given by the exponential relation

$$FP_i = A_f e^{B_f d_i} \tag{6.22}$$

where $d_i$ is the equivalent sand-grain diameter and $A$ and $B$ are coefficients.

### 6.1.2.5. Enrichment

Besides calculating the sediment transport fraction for each of the five particle size classes, the model also computes the sediment enrichment ratio based on the specific surface area of the sediment and organic matter and specific surface area for the residual soil. That is, the enrichment ratio, $ER$, is

$$ER = \frac{SSA_{sed}}{SSA_{soil}} \tag{6.23}$$

where $SSA$ is specific surface area and the subscripts 'sed' and 'soil' refer to the sediment and residual soil, respectively. As deposition of sediment occurs in transport, the organic matter, clay, and silt are the principal particles transported. This results in high enrichment ratios, important in adsorbed chemical transport.

Table 6.1. Possible elements and their calling sequence used to represent field-sized are

| Sequence Number | Elements and their Sequence |
|---|---|
| 1 | Overland |
| 2 | Overland-Pond |
| 3 | Overland-Channel |
| 4 | Overland-Channel-Channel |
| 5 | Overland-Channel-Pond |
| 6 | Overland-Channel-Channel-Pond |

#### 6.1.2.6. Watershed Elements

Every model is a representation and a simplification of the prototype. Various techniques, including planes and channels (Li, 1977), square grids (Beasley *et al.*, 1977), converging sections (Smith, 1977), and stream tubes (Onstad and Foster, 1975) have been used. Most erosion-sediment yield models have adequate degrees of freedom to fit observed data. Some models, depending on their representation scheme, distort parameter values more than others do. Distortion of parameter values greatly reduces the transferability of parameter values from one area to another (Lane *et al.*, 1975). An objective in this model development was to represent the field in a way that minimizes parameter distortion.

Overland flow, channel flow, and impoundment (pond) elements are used to represent major features of a field. The user selects the best combination of elements to represent the field and enters the appropriate sequence according to Table 6.1. The model (computer program) calls the elements in the proper sequence. Typical systems that the model can represent are illustrated in Figure 6.1.

Computations begin in the uppermost element, which is always the overland flow element, and proceed downstream. Sediment concentration (for each particle type) is the output from each element and becomes the input to the next element in the sequence.

### 6.1.3. APPLICATIONS

#### 6.1.3.1. Overland Flow

The overland flow component has been tested using data from several agricultural areas of the United States. The erosion relationships in the overland flow element gave good results for a watershed at Treynor, Iowa. Estimates were considerably better than those from the USLE using storm EI (Foster *et al.*, 1977) and better than those obtained from a procedure using runoff volume and peak discharge alone as an erosivity factor (Onstad *et al.*, 1976) in the USLE. Both rainfall and runoff seem to be important for estimating detachment on overland flow areas.

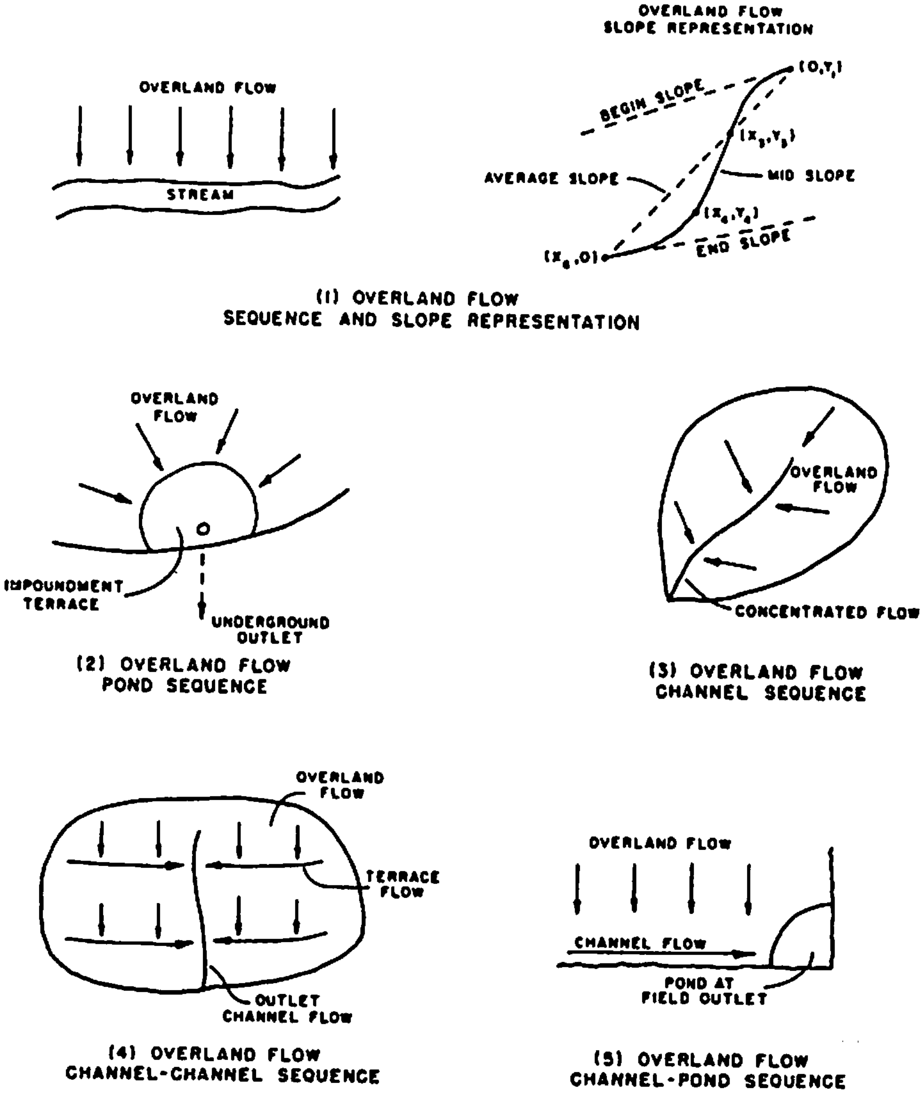


Figure 6.1 Schematic representation of typical field systems in the field-scale erosion/sediment model

More comprehensive models like ARM (Donigian and Crawford, 1976) or ANSWERS (Beasley *et al.*, 1977) use modifications of the USLE or require data for calibration or both. Our model preserves the USLE form when simulated over a range of slopes, lengths, and storms. For long-term simulation, our model produces results comparable to those of the USLE. Information to select overland flow erosion parameters is as readily available for this model as it is for the USLE.

The validity of the model has been partially assessed by comparing output with observed data and by comparing this model with other models. Output from the model has been compared with measured sediment yield from concave field plots under simulated rainfall, single terrace watersheds, small watersheds with impoundment terraces, and a small watershed with conservation tillage. The simulations were made using measured rainfall and runoff values. Parameter values were selected from the *User's Manual* (Foster *et al.*, 1980) without calibration, except as noted.

Three concave plots 10.7 m long were carefully shaped in a soil where soil properties were uniform with depth. Slope along the plots continuously decreased from 18 per cent at the upper end to 0 per cent at the lower end. Simulated rainfall at 64 mm $hr^{-1}$ was applied to one of the plots, and deposition was observed to begin 7 m from the upper end. Plot ends were installed at 7.0 and 8.8 m on the other two plots. The measured particle size distribution was used, and the soil erodibility factor and Manning's *n* were adjusted in the model to give the observed soil loss and particle size distribution for the 7.0 m plot. The estimated sediment yield for the 8.8 m plot was 3.9 g $m^{-1}$ $sec^{-1}$ compared with 2.5 g $m^{-1}$ $sec^{-1}$ observed. For the 10.7 m plot, the estimated and observed values were 1.7 and 1.4 g $m^{-1}$ $sec^{-1}$. Calculated and observed particle size distributions are shown in Table 6.2.

### 6.1.3.2. More Complex Watersheds

Soil loss was simulated for 8 years of data from small, single-terrace watersheds at Guthrie, Oklahoma (Daniel *et al.*, 1943). The simulations were made without calibration, and represented trends in the observed data quite well (Table 6.3).

Soil loss was simulated for six selected storms representing a range of rainfall and runoff characteristics for the Eldora, Charles City, and Guthrie Center, Iowa locations from an impoundment terrace study (Laflen *et al.*, 1978). The model was run using the *User Manual* instructions without calibration. Observed and computed sediment yield data for the three impoundment terraces are shown in Table 6.4. In the Julian data column, the first two digits represent the data year, and the last three digits represent the date in days since the first of the year.

Simulations were run without calibrating for about two-and-a-half years of data from the 1.3-ha P2 watershed at Watkinsville, Georgia in a conservation tillage system for corn (Smith *et al.*, 1978). Deposition in the backwater from the flume at the watershed outlet was modelled. Deposition measured in the flume backwaters was about equal to the measured sediment yield on a similar nearby watershed (Langdale *et al.*, 1979). The computed total sediment yield for the period of record was 1.47 kg $m^{-2}$, while the measured value was 1.85 kg $m^{-2}$.

### 6.1.3.3. Channel Morphology Model

The procedures described earlier were applied to data from an experimental rill erosion study at Lafayette, Indiana. The procedure was to measure channel (rill)

Table 6.2. Calculated and observed particle size distribution, in per cent, for transport of soil aggregates on concave field plots under simulated rainfall

| Plot | | Aggregate Size (μm) | | | | | | | | | |
|---|---|---|---|---|---|---|---|---|---|---|---|
| Length | Slope at end | <2 | | 2–210 | | 210–500 | | 500–1000 | | >1000 | |
| | | Ob | Cal | Ob | Cal | Ob | Cal | Ob | Cal | Ob | Cal |
| 8.8 m | 3% | 7 | 8 | 53 | 58 | 7 | 24 | 12 | 9 | 21 | 1 |
| 10.7 m | 0% | 10 | 19 | 79 | 80 | 8 | 1 | 1 | 0 | 2 | 0 |

Table 6.3. Comparison of simulated sediment yield from single terrace watersheds with measured values

| Terrace | Grade | Sediment Yield | |
|---|---|---|---|
| | | Simulated | Observed |
| | | ($kg\ m^{-2}$) | ($kg\ m^{-2}$) |
| 2B | Variable, 0.0033 at outlet to 0.0 at upper end | 6.4 | 12.2 |
| 3B | Variable, 0.005 at outlet to 0.0 at upper end | 11.9 | 13.8 |
| 3C | Constant, 0.005 | 10.6 | 12.1 |
| 5C | Constant, 0.0017 | 4.6 | 4.8 |

cross sections, flow variables, and sediment yield under controlled conditions. A non-erodible boundary at the depth of disking was present below the soil surface.

Comparisons of observed and computed sediment yields with time showed a good fit using the simplified model. Total sediment yields over the seven replicated runs produced a relation between observed sediment yields $Q_s$, and computed sediment yield $\hat{Q}_s$ as:

$$\hat{Q}_s = -11.0 + 0.93\, Q_s \qquad (6.24)$$

with an $R^2 = 0.97$. Therefore, the simplified model reproduces observed sediment yields within measurement accuracy.

In the rill erosion studies, discharge, slope, and Manning's $n$ values were measured. However, to apply the model to selected discharge-width data from the literature, it was necessary to estimate the $n$ values (Barnes, 1967). Given these estimates, the model was used to compute final widths, $W_f$, and these were compared with measured

Table 6.4. Summary of observed and simulated sediment yield from impoundment terraces in Iowa

| Watershed | Area (ha) | Julian date | Observed sediment field (kg) | Computed sediment field (kg) |
|---|---|---|---|---|
| Charles City | 1.9 | 70147 | 542 | 24 |
| | | 70152 | 33 | 6 |
| | | 70244 | 2 | 72 |
| | | 70323 | 26 | 2 |
| | | 71151 | 127 | 133 |
| | | 71157 | 95 | 72 |
| Eldora | 0.73 | 68198 | 128 | 68 |
| | | 68220 | 26 | 25 |
| | | 69187 | 479 | 251 |
| | | 69232 | 56 | 103 |
| | | 71163 | 152 | 63 |
| Guthrie Center | 0.57 | 69207 | 116 | 124 |
| | | 69249 | 10 | 40 |
| | | 70144 | 55 | 29 |
| | | 70162 | 90 | 56 |
| | | 70167 | 10 | 13 |
| | | 70229 | 5 | 24 |

values. Osterkamp (1977) selected several streams in the mountains and high plains of the United States and related channel width to a characteristic discharge. Observed and computed data for Osterkamp's 32 streams and the 7 rills are shown in Figure 6.2. Widths and discharges were then related by regression of the form

$$W = aQ^b \tag{6.25}$$

following the procedure outlined by Leopold and Miller (1956). The regression results for the observed and computed channel widths are shown in Figure 6.2. For the data from the experimental rill study, the coefficients and exponents in equation (6.25) are quite similar. Again, these results are for small rills under controlled experimental conditions. For natural streams, the exponent $b$ was larger for the computed than for the observed widths. In these wide, natural streams, the distribution of shear stress around the channel cross section may be more uniform and nearer to the average shear stress over the wetted perimeter than is assumed in the small rills. Nonetheless, as shown in Figure 6.2, the model produced a reasonable approximation to the observed width-discharge relationship.

The concept of a quasi-steady state channel developed in a homogeneous soil due to a constant discharge is an oversimplification of processes occurring in natural channels. However, the simplified model described here does seem to explain width-

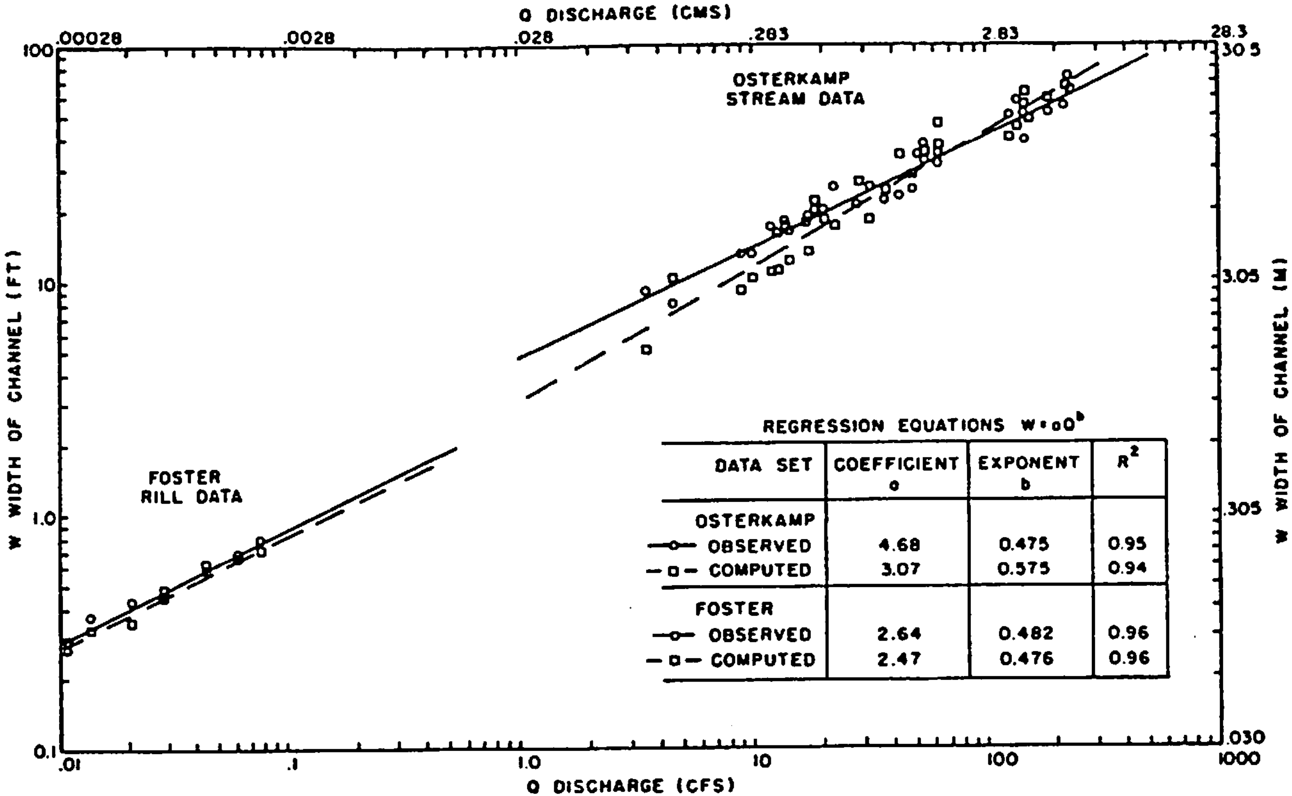


Figure 6.2 Relation between channel discharge and width for natural streams and experimental rill systems

discharge relationships that have been empirically derived over the past few decades (e.g. Leopold and Miller, 1956; Osterkamp, 1977). Moreover, width-discharge equations such as equations (6.16) and (6.18) seem to be an improvement over multiple linear regression equations used to predict channel width using discharge and other 'independent' variables. There is a hydraulic basis for the functional form in equations (6.16) and (6.18), whereas multiple linear regression equations can result from spurious correlations.

### 6.1.3.4. Selection of Best Management Practices

The model may be used to evaluate sediment yield from field-sized areas under various management practices to control nonpoint-source pollution. Given basic inputs that represent a specific field and the rainfall, the model is run to evaluate the various practices by using parameter values that characterize each specific practice. Results for such simulation runs are shown in Table 6.5. The field selected for this analysis had a typical slope length of 50 m on a uniform 6 per cent slope with a moderately erodible soil in continuous corn. The soil was assumed to be quite sandy. The analysis considered only 14 storms occurring over a two-month period around seedbed time. Several cropping years would be considered in a more complete analysis.

Practice 1 in Table 6.5 is a baseline with its uniform slope and clean tillage with no conservation practices. Practice 2 represents the effect of deposition on the toe of the concave portion of a highly convex–concave profile having an average 6 per cent slope. This is really not a management practice, since topography generally cannot be radically changed. Practice 3 shows that deposition in two grass strips along a uniform slope, one in the middle and one at the toe, can significantly reduce sediment yield. Difficulties in uniformly constructing and maintaining the strip may in practice greatly reduce their effectiveness. Practices 4, 5, and 6 represent the effect of concentrated flow in a field. The difference between Practices 1 and 4 is due to erosion by concentrated flow. A well constructed grass waterway eliminates that erosion and traps sediment coming from overland flow areas. Ponding at the field outlet can also reduce sediment yield, as Practice 5 shows.

Conventional terraces effectively control erosion and sediment yield when properly installed. If their grades are too steep, as in Practice 7, they erode. On a flat grade as in Practice 10, they do not erode, but trap significant amounts of sediment. The delivery ratio of terraces is not constant, as frequently assumed. Impoundment terraces very effectively control sediment yield in many circumstances, as illustrated by Practice 11.

Practices 12 to 15 are cultural practices frequently referred to as conservation tillage. Their effectiveness mainly depends on surface cover of residue from the previous year's crop. Finally, Practices 16 and 17 show the influence of combining terraces with conservation tillage practices. The relative effectiveness of such structures varies with the tillage practice.

Table 6.5. Typical best management that can be analysed with the model and typical sediment yield estimates

| Practice | All 14 storms | | Small storm $EI = 6.1\ (kJ\ ha^{-1}) \cdot (mm\ hr^{-1})$ Runoff = 2.8 mm | | Large storm $EI = 77.3\ (kJ\ ha^{-1}) \cdot (mm\ hr^{-1})$ Runoff = 44.2 mm | |
|---|---|---|---|---|---|---|
| | Sediment yield ($t\ ha^{-1}$) | Computed delivery ratio | Sediment yield ($t\ ha^{-1}$) | Computed delivery ratio | Sediment yield ($t\ ha^{-1}$) | Computed delivery ratio |
| 1 Conventional | 29.5 | 1.00[a] | 0.5 | 1.00[a] | 23.8 | 1.00[a] |
| 2 Conventional, complex slope w/concave at toe | 5.1 | 0.17[a] | 0.0 | 0.05[a] | 4.8 | 0.20[a] |
| 3 Stripcropping, grass buffer strip | 1.7 | 0.06[a] | 0.0 | 0.00[a] | 1.6 | 0.07[a] |
| 4 Conventional, concentrated flow | 36.7 | 1.24[a] | 0.5 | 1.00[a] | 28.4 | 1.19[a] |
| 5 Conventional, concentrated flow, restricted outlet | 27.8 | 0.94[a] | 0.3 | 0.67[a] | 22.5 | 0.94[a] |
| 6 Conventional, grass waterway | 12.1 | 0.41[a] | 0.1 | 0.24[a] | 10.5 | 0.44[a] |
| 7 Conventional, 12.5 m terr. int., 1% grade | 22.1 | 0.75[b] | 0.2 | 0.48[b] | 19.9 | 0.84[b] |

| | | | | | | |
|---|---|---|---|---|---|---|
| 8 Conventional, 12.5 m terr. int., 0.8% grade | 15.7 | 0.53[b] | 0.2 | 0.48[b] | 13.7 | 0.57[b] |
| 9 Conventional, 12.5 m terr. int., 0.5% grade | 10.4 | 0.35[b] | 0.2 | 0.48[b] | 8.5 | 0.36[b] |
| 10 Conventional, 12.5 m terr. int., 0.25% grade | 6.4 | 0.22[b] | 0.1 | 0.24[b] | 5.3 | 0.22[b] |
| 11 Conventional, impoundment terr. | 0.4 | 0.02[b] | 0.0 | 0.03[b] | 0.3 | 0.01[b] |
| 12 Chisel, 5000 kg $ha^{-1}$, 50% cover | 5.2 | – | 0.0 | – | 4.8 | – |
| 13 Chisel, 2000 kg $ha^{-1}$, 20% cover | 13.2 | – | 0.2 | – | 11.9 | – |
| 14 No till, 5000 kg $ha^{-1}$, 80% cover | 2.1 | – | 0.0 | – | 1.9 | – |
| 15 No till in killed sod | 0.3 | – | 0.0 | – | 0.3 | – |
| 16 Chisel, 2000 kg $ha^{-1}$, 20% cover, 12.5 m terr., 0.5% grade | 5.4 | 0.41[b] | 0.0 | 0.09[b] | 4.9 | 0.41[b] |
| 17 No till, 5000 kg $ha^{-4}$, 80% cover, 12.5 m terr., 0.5% grade | 2.9 | 1.41[b] | 0.0 | 0.08[b] | 2.7 | 1.47[b] |

[a] Ratio of sediment yield at outlet to sediment yield from uniform slope, conventional management.
[b] Ratio of sediment yield at terrace outlet to sediment yield from uniform slope with no terraces. Slope length and steepness = 50 m and 6%, respectively. Corn at seedbed time.

If 7 t ha$^{-1}$ is an allowable sediment yield, eight of the 17 practices in Table 6.5 (excluding the topographic effect of the concave slope of Practice 2) adequately control sediment yield, so one can choose a practice from these eight which would best fit the particular farming operation. The relative, and certainly the absolute results, are unlikely to be the same under different farming conditions at other locations. Nonetheless, this simulation study illustrates the intended use of the model described herein, for it provides a means of evaluating alternative management practices with respect to their relative influence on sediment yield for a given location with specified characteristics of climate, topography, soils, etc.

## 6.1.4. SUMMARY

An erosion-sediment yield model for field-sized areas is developed for use on a storm-by-storm basis. Our overall objective is to develop a model, incorporating fundamental erosion-sediment transport relationships, to evaluate best management practices. Although the procedure does not consider changes in parameter values within individual storms, it does allow these parameters to change from storm to storm throughout the season. However, parameters of the model allow for distribution of field characteristics along overland flow slopes and waterways. Many of the model parameters are selected using tested methods developed for the well known Universal Soil Loss Equation. For this reason, we feel that the model has immediate applications without extensive calibration.

Limited testing has shown that the procedures developed here give improved estimates over the USLE and modified USLE procedures. We tested specific components of the model using experimental data from overland flow, erodible channel, and impoundment studies. Testing and sensitivity analyses are described elsewhere. Initial results suggested that the model produces reasonable results and is a powerful tool for analyzing the influence of alternative management practices.

A simple model has been developed to compute channel widths and associated erosion rates or sediment yields with time for eroding channels. The model reproduced observed sediment yield data from an experimental rill erosion study. The quasi-steady state width-discharge relationships predicted by the simple model compared well with observed data from natural channels.

## 6.1.5. ACKNOWLEDGEMENTS

The authors wish to thank the USDA-SEA-AR, Lafayette, Indiana, and Southwest Watershed Research Center, Tucson, Arizona for their support.

## REFERENCES

Barnes, H. H., 1967, Roughness characteristics of natural channels, *US Geological Survey Water Supply Paper 1849*, 213 pp.

Beasley, D. B., Monke, E. J., and Huggins, L. F., 1977, The ANSWERS model: A planning tool for watershed research, *Paper No. 77-2532*, American Society of Agricultural Engineers, St. Joseph, Michigan.

Chow, V. T., 1969, *Open-Channel Hydraulics*, McGraw-Hill Book Company, Inc., New York, NY, 680 pp.

Daniel, H. A., Elwell, H. M., and Cox, M. B., 1943, Investigations in erosion control and reclamation of eroded land at the Red Plains Conservation Experiment Station, Guthrie, Oklahoma, 1930–1940, *UDSA Technical Bulletin No. 837*, 34 pp.

Davis, S. S., 1978, Deposition of nonuniform sediment by overland flow on concave slopes, *M.S. Thesis*, Purdue University, West Lafayette, Indiana.

Donigian, A. S., Jr., and Crawford, N. H., 1976, Modelling nonpoint source pollution from the land surface, *US Environmental Protection Agency*, EPA-600/376-083, 279 pp.

Einstein, H. A., 1968, Deposition of suspended particles in a gravel bed, *J. Hyd. Div., Proc. Amer. Soc. Civ. Eng.*, 94(HY5), 1197–1205.

Foster, G. R., Meyer, L. D., and Onstad, C. A., 1977, A runoff erosivity factor and variable slope length exponents for soil loss estimates, *Trans. Amer. Soc. Agric. Engrs.*, 20(4), 683–687.

Foster, G. R., Lane, L. J., and Nowlin, J. D., 1980, A model to estimate sediment yield from field sized areas: Selection of Parameter values—A field scale model for chemicals, runoff, and erosion from agricultural management systems, Conservation Research Report No 26, USDA Science and Education Administration, Vol. II, Users Manual, Chapter 2, pp. 193–281.

Knisel, W. G., 1978, A system of models for evaluating nonpoint source pollution—An overview, *International Institute for Applied Systems Analysis*, A-2361, Laxenburg, Austria, Pub. CP-78-11, 17 pp.

Laflen, J. M., Johnson, H. P., and Hartwig, R. O., 1978, Sedimentation modelling of impoundment terraces, *Trans. Amer. Soc. Agric. Engrs.*, 21(6), 1131–1135.

Lane, L. J., Woolhiser, D. A., and Yevjevich, V., 1975, Influence of simplification in watershed geometry in simulation of surface runoff, *Hydrology Paper No. 81*, Colorado State University, Fort Collins, Colorado, 50 pp.

Langdale, G. W., Barnett, A. P., Leonard, R. A., and Fleming, W. G., 1979, Reduction of soil erosion by no-till systems in the southern Piedmont, *Trans. Amer. Soc. Agric. Engrs.*, 22(1), 82–86, 92.

Leopold, L. B., and Miller, J. P., 1956, Ephemeral streams—hydraulic factors and their relation to the drainage net, *US Geological Survey Professional Paper 282-A*, 32 pp.

Li, R. M., 1977, Water and sediment routing from watersheds, *Proceedings of River Mechanics Institute*, Colorado State University, Fort Collins, Colorado, Chapter 9.

Onstad, C. A., and Foster, G. R., 1975, Erosion modelling on a watershed, *Trans. Amer. Soc. Agric. Engrs.*, 18(2), 288–292.

Onstad, C. A., Piest, R. F., and Saxton, K. E., 1976, Watershed erosion model validation for southwest Iowa, in *Proceedings of the Third Federal Interagency Sedimentation Conference*, Water Resources Council, Washington, DC, Chapter 1, pp. 22–24.

Osterkamp, W. R., 1977, Effect of channel sediment on width-discharge relations, with emphasis on streams in Kansas, *Bulletin No. 21*, Kansas Water Resources Board, 25 pp.

Smith, R. E., 1977, Field test of a distributed watershed erosion/sedimentation model, in *Soil Erosion: Prediction and Control*, Special Publication No. 21, Soil Conservation Society of America, Ankeny, Iowa, pp. 201–209.

Smith, C. N., Leonard, R. A., Langdale, G. W., and Bailey, G. W., 1978, Transport of agricultural chemicals from small upland Piedmont watersheds, *US Environmental Protection Agency* EPA-600/3-78-056, 364 pp.

Williams, J. R., 1975, Sediment-yield prediction with Universal Equation using runoff energy factor, in *Present and Prospective Technology for Predicting Sediment Yields and Sources*, ARS-S-40, USDA-Science and Education Administration, pp. 244–252.

Wischmeier, W. H., and Smith, D. D., 1978, Predicting rainfall erosion losses, *Agricultural Handbook, No. 537*, USDA-Science and Education Administration, 58 pp.

Yalin, Y. S., 1963, An expression for bedload transportation, *J. Hydr. Div. Proc. Amer. Soc. Civil Engr.*, 89(HY3), 221–250.

British Library Cataloguing in Publication Data:

Tropical agricultural hydrology.
1. Agriculture–Tropics
I. Lal, R. II. Russell, Edward Walter
III. International Institute of Tropical Agriculture
630'.913 SB111 80-41590

ISBN 0 471 27931 5

Typeset by Activity, Teffont, Salisbury, Wilts
and printed in Great Britain by The Pitman Press, Bath, Avon